



**HAL**  
open science

## Non-Gaussian diffusion near surfaces

Arthur Alexandre, Maxime Lavaud, Nicolas Fares, Elodie Millan, Yann Louyer, Thomas Salez, Yacine Amarouchene, Thomas Guérin, David S. Dean

► **To cite this version:**

Arthur Alexandre, Maxime Lavaud, Nicolas Fares, Elodie Millan, Yann Louyer, et al.. Non-Gaussian diffusion near surfaces. 2022. hal-03713580v1

**HAL Id: hal-03713580**

**<https://hal.science/hal-03713580v1>**

Preprint submitted on 4 Jul 2022 (v1), last revised 30 Nov 2022 (v3)

**HAL** is a multi-disciplinary open access archive for the deposit and dissemination of scientific research documents, whether they are published or not. The documents may come from teaching and research institutions in France or abroad, or from public or private research centers.

L'archive ouverte pluridisciplinaire **HAL**, est destinée au dépôt et à la diffusion de documents scientifiques de niveau recherche, publiés ou non, émanant des établissements d'enseignement et de recherche français ou étrangers, des laboratoires publics ou privés.

# Non-Gaussian diffusion near surfaces

Arthur Alexandre,<sup>1</sup> Maxime Lavaud,<sup>1</sup> Nicolas Fares,<sup>1</sup> Elodie Millan,<sup>1</sup> Yann Louyer,<sup>1</sup>  
Thomas Salez,<sup>1</sup> Yacine Amarouchene,<sup>1</sup> Thomas Gu erin,<sup>1</sup> and David S. Dean<sup>1,2</sup>

<sup>1</sup>*Univ. Bordeaux, CNRS, LOMA, UMR 5798, F-33400, Talence, France.*

<sup>2</sup>*Team MONC, INRIA Bordeaux Sud Ouest, CNRS UMR 5251,  
Bordeaux INP, Univ. Bordeaux, F-33400, Talence, France.*

We study the diffusion of finite-size particles confined close to a single wall and in double-wall planar channel geometries. The local diffusion constants are modified near the confining boundaries and depend on the distance to the latter. Displacement parallel to the walls is diffusive as characterized by its second cumulant (the variance), but a non-Gaussian nature can be demonstrated by the fact that its fourth cumulant is non-zero. Establishing a link with the well-known problem of Taylor dispersion, we provide a general expression for the fourth cumulant for general diffusivity tensors and also in the presence of potentials generated by either the walls or externally, for instance due to gravity. We then analyse experimentally and numerically the motion of a colloid in the direction parallel to the wall, for which the measured fourth cumulant is correctly predicted by our theory. This system is a well-controlled physical realization of a Brownian yet non-Gaussian motion generated by a fluctuating diffusivity mechanism for which the local diffusivity is quantified. These results can be used to provide additional tests and constraints for the inference of force maps and local transport properties near surfaces.

It is generally accepted that the transport properties of tracer particles in complex media can be vastly different from those observed in simple fluids. In the bulk of simple fluids, beyond molecular length and time scales, the motion of a colloidal particle satisfies two important properties: (i) its mean squared displacement (MSD) increases linearly with time (diffusive behavior) and (ii) the probability distribution functions (PDF) of position increments are Gaussian. In complex media, exhibiting dynamical and spatial heterogeneities, or in presence of flows or active forces, both properties (i) and (ii) are generally not satisfied. Examples range from non-Gaussian transport in hydrodynamic flows, with consequences for chemical delivery in microfluidic environments [1], to the wide body of experimental observations of *anomalous* diffusion in complex fluids and biological media [2–6].

Interestingly, it has recently been noted that, in a large class of complex media, the motion can be described as *Fickian yet non-Gaussian*, or *anomalous yet Brownian* [7–13]. These terms both refer to processes with linear-in-time MSDs but non-Gaussian dispersion PDFs. A generic explanation for this phenomenon was introduced in Ref. [14] via the *diffusing diffusivity* mechanism. In this scenario, Fickian yet non-Gaussian motion is generated by a fluctuating diffusion constant, arising for example from fluctuations of the local density or of the instantaneous gyration radius for complex macromolecules [15]. Properties of random walks with the diffusing diffusivity mechanism were further explored [16–22], but in most studies the assumptions invoked for the dynamically evolving diffusivity are generic but rather phenomenological. To the best of our knowledge, with the exception of the Brownian motion of an ellipsoidal particle [23, 24], there is currently no experimental realization of a there is currently no experimental realization of a system ex-

hibiting the diffusing diffusivity mechanism at all times where the local diffusivity is quantified both experimentally and theoretically over a broad spatial range.

The goal of the present Letter is to quantitatively address a model of Fickian yet non-Gaussian process by studying a tracer particle diffusing near a hard wall. In particular, we provide an exact theoretical calculation, which we verify experimentally and numerically, of the fourth cumulant of the displacement along the walls, which quantifies non-Gaussianity at all times. Indeed, due to hydrodynamic interactions, the local diffusivity in the direction parallel to the wall depends on the distance to the wall which itself fluctuates due to diffusion perpendicular to the wall. This generates the diffusing diffusivity mechanism. Note that a similar situation was previously considered in an experimental work [25] which however focused on the motion perpendicular to the wall: in this case, the non-Gaussian behavior due to diffusing diffusivity can be observed only at small times, since at long times the presence of an interaction potential with the wall induces non-Gaussian displacements - even for uniform diffusivity. Here, we concentrate on the motion parallel to the wall which is a genuine realization of diffusing diffusivity at all times. Specifically, our theoretical analysis identifies a link with standard Taylor dispersion, due to an imposed flow, and the diffusing diffusivity mechanism studied here. We also predict that fourth moment takes an explicit and simple form for narrow channels. Beyond the interest of our study as an explicit example of non-Gaussian yet Brownian motion, the characterization of the fourth cumulant is of interest to the recurrent problem of inferring map forces and local transport coefficients in heterogeneous environments [26, 27] and at the vicinity of surfaces [28].

*Physical model.* We consider a system where a Brown-

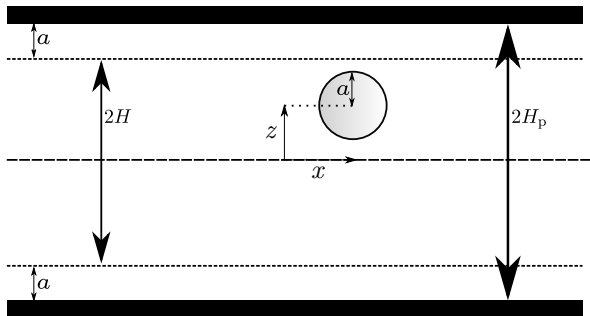


FIG. 1. Schematic of the system. A particle of radius  $a$  diffuses in two dimensions, between two walls separated by a distance  $2H_p$ .

ian particle of radius  $a$  is confined between two walls separated by a distance  $2H_p$ , as shown in Fig. 1. The particle diffuses along the channel (*i.e.* the  $x$ -axis) and perpendicularly to it (*i.e.* the  $z$ -axis) with respective height-dependent diffusion coefficients  $D_{\parallel}(z)$  and  $D_{\perp}(z)$ . The particle is subject to a potential  $V(z)$ , and the probability density  $p(z, t)$  about  $z$  at time  $t$  thus obeys the Fokker-Planck equation  $\partial_t p = -\mathcal{H}p(z, t)$ , where

$$\mathcal{H} = -\frac{\partial}{\partial z} \left\{ D_{\perp}(z) \left[ \frac{\partial}{\partial z} \cdot + \beta V'(z) \right] \right\}, \quad (1)$$

with  $\beta = 1/(k_B T)$ , where  $k_B$  is Boltzmann's constant and  $T$  the temperature. We assume no-flux conditions at the walls. In the long-time limit, the system equilibrates along the  $z$  direction and attains a Gibbs-Boltzmann distribution (see Fig. 2(a)) denoted by

$$p_0(z) = \frac{\exp(-\beta V(z))}{\int_{-H}^H dz' \exp(-\beta V(z'))}. \quad (2)$$

We denote by  $Z_t \in [-H, H]$  the height of the center of the particle at time  $t$ , and  $H = H_p - a$  is the effective channel height available to the particle. In addition,  $X_t$  denotes the position of the center of the particle along the channel. Our goal is to characterize transport properties along the channel, which we quantify by the second and fourth order cumulants:

$$\langle X_t^2 \rangle_c \equiv \langle X_t^2 \rangle, \quad \langle X_t^4 \rangle_c \equiv \langle X_t^4 \rangle - 3\langle X_t^2 \rangle^2, \quad (3)$$

where  $\langle \cdot \rangle$  denotes the ensemble average, and the initial condition is  $X_{t=0} = 0$ , while  $Z_{t=0}$  is assumed to be drawn from the distribution  $p_0$ . The quantity  $\langle X_t^4 \rangle_c$  vanishes if  $X_t$  is Gaussian, therefore its evaluation is the simplest way to quantify the non-Gaussianity of the process  $X_t$ .

*General theory.* Since  $X_t$  is not subject to a potential, its trajectories are governed by the stochastic differential equation

$$dX_t = \sqrt{2D_{\parallel}(Z_t)} dB_{x,t}, \quad (4)$$

where the Gaussian increments  $dB_{x,t}$  have zero average and  $\langle dB_{x,t}^2 \rangle = dt$ . In Eq. (4), we will use the Ito prescription of the stochastic calculus, however the fact that  $D_{\parallel}(Z_t)$  is independent of  $X_t$  means that this choice is unimportant. Integrating Eq. (4) gives

$$X_t = \int_0^t \sqrt{2D_{\parallel}(Z_{\tau})} dB_{x,\tau}. \quad (5)$$

Squaring this and using the independence of  $dB_{x,t}$  and  $Z_t$ , then taking the average assuming that the process  $Z_t$  has equilibrated, yields an expression for the MSD:

$$\langle X_t^2 \rangle_c \equiv \langle X_t^2 \rangle = 2t \int_{-H}^H dz D_{\parallel}(z) p_0(z) = 2 \langle D_{\parallel} \rangle_0 t, \quad (6)$$

where  $\langle \cdot \rangle_0$  denotes the average with respect to the equilibrium distribution  $p_0(z)$ . We thus note that the MSD is linear in time at all times, so that  $X_t$  is a physical example of non-Gaussian yet Brownian stochastic process. We note that the MSD is independent of the precise dynamics of the process  $Z_t$  and only depends on its equilibrium distribution, as such it contains no information about its correlations. Next, taking the fourth-power of Eq. (5) and evaluating the resulting integrals by using Wick's theorem leads to a formal expression for the fourth-order cumulant [29]

$$\frac{\langle X_t^4 \rangle_c}{12} = \int_0^t ds \int_0^t ds' [\langle D_{\parallel}(Z_s) D_{\parallel}(Z_{s'}) \rangle - \langle D_{\parallel} \rangle_0^2]. \quad (7)$$

At this stage, we notice an analogy with the well-established theory of Taylor-dispersion, which quantifies the dispersion of particles in channels in presence of hydrodynamic flows. We imagine the same process  $Z_t$  but consider the a convective displacement given along the channel by

$$dY_t = u(Z_t) dt, \quad Y_t = \int_0^t ds u(Z_s), \quad (8)$$

where  $u(z)$  is an arbitrary imposed flow field along the channel. Evaluating the first cumulants of  $Y_t$  in this, Taylor-dispersion, problem yields

$$\langle Y_t \rangle_c = \langle u \rangle_0 t, \quad (9)$$

$$\begin{aligned} \langle Y_t^2 \rangle_c &= \langle Y_t^2 \rangle - \langle Y_t \rangle^2 \\ &= \int_0^t ds \int_0^t ds' [\langle u(Z_s) u(Z_{s'}) \rangle - \langle u \rangle_0^2]. \end{aligned} \quad (10)$$

Comparing the above expressions with Eqs. (6) and (7) makes clear that the second and fourth cumulants of  $X_t$  are proportional to the average and the variance of  $Y_t$  in a Taylor dispersion problem with the formal correspondence  $u(z) = D_{\parallel}(z)$ . This analogy also shows that  $\langle X_t^4 \rangle_c$  is always positive (since it is up to a positive numerical prefactor equal to the variance for the

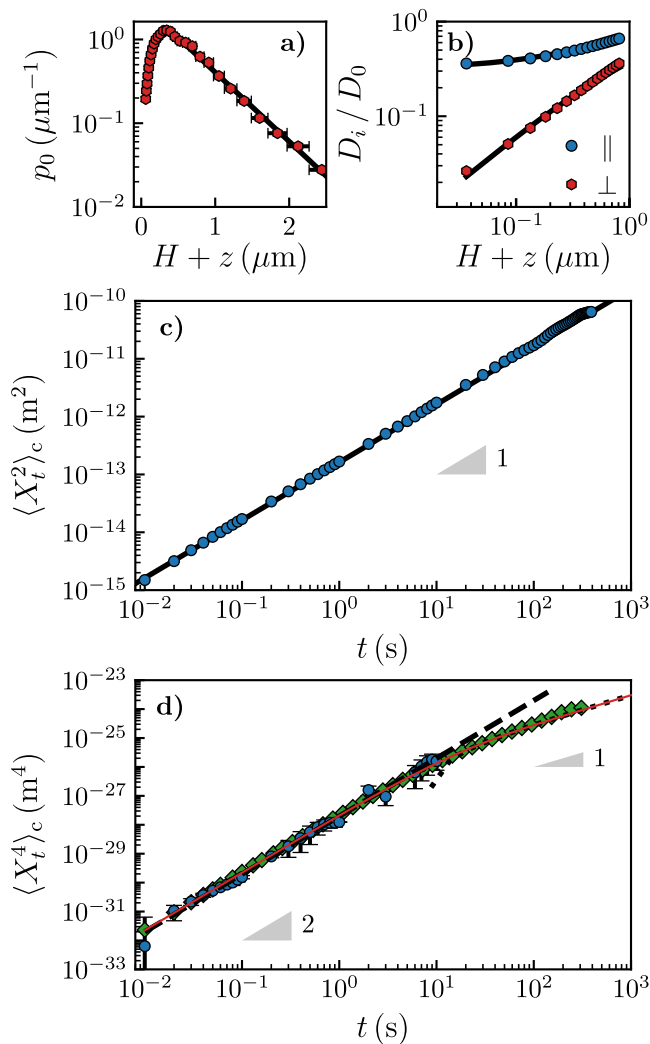


FIG. 2. (a) Experimentally-measured long-time probability density function  $p_0(z)$  in position  $z$ , as a function of the distance  $H+z$  to the bottom wall. The solid line represents the best fit to the normalized Gibbs-Boltzmann distribution of Eq. (2), using the potential  $V(z)$  defined in Eq. (19) with  $B = 5.0$ ,  $l_D = 88$  nm and  $l_B = 526$  nm, and at room temperature. (b) Experimentally-measured horizontal ( $i = \parallel$ ) and vertical ( $i = \perp$ ) local diffusion coefficients  $D_i(z)$ , normalized by the bulk value  $D_0$ , as functions of the distance  $H+z$  to the bottom wall. The solid lines represent the theoretical predictions  $D_i(z) = k_B T / [6\pi a \mu_i(z)]$  using Eqs. (20) and (21). (c) Experimentally-measured second cumulant  $\langle X_t^2 \rangle_c$  of the horizontal displacement as a function of time  $t$ . The solid line corresponds to Eq. (6), with  $\langle D_{\parallel} \rangle_0 = 0.58 D_0$ . The slope triangle indicates an exponent 1. (d) Experimentally-measured (blue dots) and numerically-simulated (green diamonds) fourth cumulant  $\langle X_t^4 \rangle_c$  of the horizontal displacement as functions of time  $t$ . The solid line represents the theoretical expression of Eq. (11), while the dashed and dotted lines are the asymptotic expressions at short and long times, respectively, as given by Eqs. (12) and (13), with no adjustable parameter. The slope triangles indicate exponents 2 and 1.

Taylor-dispersion problem). Furthermore, this analogy shows that  $\langle X_t^4 \rangle_c \propto t$  at long times. As such the non-Gaussianity parameter, known as normalized kurtosis,  $\alpha(t) \equiv \langle X_t^4 \rangle_c / \langle X_t^2 \rangle_c^2 \propto 1/t$  at late times.

Taylor dispersion has been widely studied analytically [30–40] and we can exploit existing results for the MSD at all times from Ref. [40], yielding the explicit expression:

$$\begin{aligned} \langle X_t^4 \rangle_c &= 24 \int_{-H}^H dz \int_{-H}^H dz' D_{\parallel}(z) D_{\parallel}(z') p_0(z') \\ &\times \sum_{\lambda > 0} \left[ \frac{t}{\lambda} - \frac{1 - e^{-\lambda t}}{\lambda^2} \right] \psi_{R\lambda}(z) \psi_{L\lambda}(z'), \end{aligned} \quad (11)$$

where  $\psi_{R\lambda}(z)$  and  $\psi_{L\lambda}(z)$  respectively denote the right and left eigenfunctions of  $\mathcal{H}$ , with eigenvalue  $\lambda$ , with the normalization  $\int_{-H}^H dz \psi_{L\lambda}(z) \psi_{R\lambda}(z) = 1$ . In practice, this general expression can be evaluated by numerically computing the eigenfunctions (after discretizing the operator  $\mathcal{H}$ ). This formula further simplifies at short times, where we find [29]

$$\langle X_t^4 \rangle_c \underset{t \rightarrow 0}{\simeq} 12 t^2 \left[ \langle D_{\parallel}^2 \rangle_0 - \langle D_{\parallel} \rangle_0^2 \right]. \quad (12)$$

This quadratic behavior with time implies that at short times the non-Gaussianity parameter  $\alpha(t=0)$  is finite and is simply proportional to the variance of  $D_{\parallel}(z)$  with respect to the equilibrium distribution, as in [14]. The late-time behavior can be similarly simplified yielding

$$\langle X_t^4 \rangle_c \underset{t \rightarrow +\infty}{\simeq} 24 (D_4 t - C_4), \quad (13)$$

where the explicit integral expression of  $C_4$  is given in [29], and where:

$$D_4 = \left\langle \frac{(J \exp(\beta V))^2}{D_{\perp}} \right\rangle_0, \quad (14)$$

with:

$$J(z) = \int_{-H}^z dz' \exp(-\beta V(z')) [D_{\parallel}(z') - \langle D_{\parallel} \rangle_0]. \quad (15)$$

*Approximate strong confinement theory.* To illustrate a simple application of Eq. (11), we consider the case where the channel is sufficiently narrow with respect to the particle size, so that the local diffusion coefficients can be approximated by the quadratic expressions [41, 42]:

$$\begin{cases} D_{\perp}(z) \approx D_{\perp 0} \left( 1 - \frac{z^2}{H_s^2} \right), \\ D_{\parallel}(z) \approx D_{\parallel 0} \left( 1 - \frac{z^2}{H_s^2} \right), \end{cases} \quad (16)$$

where  $H_s$  is a characteristic distance that can be considered as a slip-like length if  $H_s > H$ . The coefficients  $D_{\perp 0}$  and  $D_{\parallel 0}$  depend on the effective channel height  $H$

and on the particle radius  $a$ . In principle, the non-slip boundary condition must impose that  $D_{\parallel}(z)$  is zero at the walls, which would imply that  $H_s = H$ , however numerically  $D_{\parallel}(z)$  is found to be quadratic near the channel center and decays rapidly to zero near the walls [42]. For simplicity, and to obtain explicit analytical results, we consider no external potential. In this case, Eq. (11) can be evaluated by noting that the eigenfunctions are the Legendre polynomials  $P_n(z/H)$  of degree  $n$ , with the associated eigenvalues

$$\lambda_n = \frac{D_{\perp 0}}{H^2} n(n+1). \quad (17)$$

Expressing  $D_{\parallel}(z)$  in terms of Legendre polynomials, one obtains the full temporal behavior of the fourth cumulant:

$$\frac{\langle X_t^4 \rangle_c}{24} = \frac{2D_{\parallel 0}^2 H^6 t}{135D_{\perp 0} H_s^4} - \frac{D_{\parallel 0}^2 H^8 [1 - \exp(-\frac{6D_{\perp 0} t}{H^2})]}{405D_{\perp 0}^2 H_s^4}. \quad (18)$$

Interestingly, for this model there is only one relaxation time, equal to the time for the particle to diffuse perpendicularly. This result can be generalized to arbitrary forms for  $D_{\parallel}(z)$ , keeping the same form of  $D_{\perp}$  [29], in which case many relaxation times appear. At short times, the non-Gaussianity parameter reads  $\alpha(0) = (12H^4)/(5(3H_s^2 - H^2)^2)$  and is thus of order one. For instance if one takes  $H_s = H$  then  $\alpha(0) = 3/5$ .

*Experimental system.* We now describe an experimental observation of the non-Gaussian yet Brownian motion of a colloidal particle near a wall. In our experiments, a polystyrene particle, with radius  $a = 1.519 \pm 0.009 \mu\text{m}$  diffuses in an aqueous NaCl solution confined between two glass walls. Its trajectory is three-dimensionally tracked using Mie holography [43]. Here,  $H_p = 40 \mu\text{m}$ , so that  $H_p \gg a$ . In addition, the density mismatch of the particle is chosen such that the particle is visibly localized near the lower wall due to gravity (see Fig. 2(a)). So, the effect of the upper wall is negligible both in terms of hydrodynamic and conservative forces.

Using the mean-field theory of electrolytes [44], and taking into account the density mismatch  $\Delta\rho$  between the polystyrene bead and the solution, the dimensionless total energy potential reads:

$$\beta V(z) = B \exp\left(-\frac{H+z}{l_D}\right) + B \exp\left(-\frac{H-z}{l_D}\right) + \frac{z}{l_B}. \quad (19)$$

The first two terms account for the screened electrostatic interactions between the negatively-charged surfaces of the walls and the bead, where  $l_D$  is the Debye length and  $B$  is a dimensionless number depending in particular on the wall and bead surface charges. We have used the superposition approximation, valid for gaps large compared to  $l_D$  so that the two potentials can be simply

summed. The second term accounts for gravity, where  $l_B = k_B T / (\frac{4}{3}\pi a^3 \Delta\rho g)$ , with  $g$  the gravitational acceleration, is the Boltzmann length which indicates how far the bead can typically be from the lower wall. Equations (2) and (19) are used to fit the experimentally measured equilibrium distribution  $p_0(z)$ . The agreement is good with  $B = 5.0 \pm 0.3$ ,  $l_D = 88 \pm 2 \text{ nm}$  and  $l_B = 526 \pm 5 \text{ nm}$ , as shown in Fig. 2(a). Specifically, assuming a perfect sphere, the value of  $l_B$  gives a density mismatch  $\Delta\rho = 53 \text{ kg/m}^3$ , which is within 5% error compared to the tabulated value of  $50 \text{ kg/m}^3$ .

Moving on to hydrodynamic interactions, the local diffusion constants  $D_{\parallel}$  and  $D_{\perp}$  are inferred from the experimentally observed trajectories [43] [29] and shown in Fig. 2(b). The results agree with the Stokes-Einstein relations  $D_i(z) = k_B T / [6\pi a \mu_i(z)]$ , where  $i \in \{\parallel, \perp\}$  ( $\parallel = x, y$ ), and where  $\mu_i$  are the components of an effective viscosity tensor [45]. These components were derived previously for a single sphere close to a flat solid surface. The transverse component reads [46]:

$$\mu_{\parallel}(z) = \mu_0 \left(1 - \frac{9}{16}\xi + \frac{1}{8}\xi^3 - \frac{45}{256}\xi^4 - \frac{1}{16}\xi^5\right)^{-1}, \quad (20)$$

with  $\xi = a/(z + H_p)$ , and where  $\mu_0$  is the bulk viscosity. The normal component was derived in [45] as an infinite sum which can be Padé-approximated within 1% numerical accuracy [47], to:

$$\mu_{\perp}(z) = \mu_0 \frac{6(z+H)^2 + 9a(z+H) + 2a^2}{6(z+H)^2 + 2a(z+H)}. \quad (21)$$

These expressions, through the associated diffusion coefficients, are in agreement with the experimental data at room temperature and with  $\mu_0 = 1 \text{ mPa}\cdot\text{s}$  for water, as shown in Fig. 2(b). Combined with the previously-mentioned equilibrium properties (see Eq. (19)), they can thus be used as inputs to compute the theoretical values of the fourth cumulant of  $X_t$ .

*Comparison with theory.* Experimentally, the displacements  $X_t$  are used to estimate  $\langle X_t^2 \rangle_c$  and  $\langle X_t^4 \rangle_c$ , computed using the method of sliding averages described in [29] and leading to Figs. 2(c,d). First, the effective diffusion constant,  $\langle D_{\parallel} \rangle_0$  defined in Eq. (6), is given numerically by  $\langle D_{\parallel} \rangle_0 = 0.58 D_0$ , where  $D_0 = k_B T / (6\pi a \mu_0)$  is the bulk diffusion constant. This is in agreement with the experimental data shown in Fig. 2(c). Secondly, the short-time theoretical prediction in Eq. (12) correctly predicts the experimental data of  $\langle X_t^4 \rangle_c$  with no adjustable parameter (see Fig. 2(d)). Lack of data at long times makes it difficult to check the late-time prediction given by Eq. (13). This result can however be verified through numerical simulations, as shown in Fig. 2(d), where the simulation details are given in [29]. The whole range of experimental and numerical data can be reproduced, up to error bars, by the exact prediction of Eq. (11), where the eigenfunctions and

eigenvalues of  $\mathcal{H}$  are computed numerically. Beyond validation of the theoretical predictions, our experiments thus confirm that the system studied is a physically realizable, and well characterized example of a non-Gaussian diffusive process that nevertheless displays a linear MSD at all times, for which the non-Gaussianness is explicitly linked to the local diffusivity.

*Conclusion.* In this Letter, we have addressed theoretically, experimentally and numerically, a canonical physical realization of the diffusing diffusivity scenario at all times. We have established a mapping onto Taylor dispersion, where the diffusivity is formally replaced by a flow field. Such a mapping implies that the fourth cumulant must be positive (thus the PDF of displacements displays heavier tails than a Gaussian distribution) and linear at long times. This analogy also enables us to provide quantitative predictions characterizing dispersion along the channel. The predictions agree with experimental and numerical data, with no additional fitting parameter apart from the physical ones obtained independently in the experiments. It is interesting to note that the effective diffusion constant along the channel only depends on the equilibrium properties of the process normal to the wall,  $Z_t$ , and is otherwise independent of its dynamics, the fourth cumulant depends on the precise details of dynamics via the appearance of the two-point probability density functions. The fourth cumulant thus carries extra information on the dynamics and as such, appears to be a key statistical observable that can further contribute to improve the experimental resolution for the inference of force maps and local transport properties near surfaces.

## ACKNOWLEDGMENTS

The authors acknowledge financial support from the Agence Nationale de la Recherche (ANR) under EMetBrown (ANR-21-ERCC-0010-01), Softer (ANR-21-CE06-0029), Fricolas (ANR-21-CE06-0039) and ComplexEncounters (ANR-21-CE30-0020) grants. They thank the Soft Matter Collaborative Research Unit, Frontier Research Center for Advanced Material and Life Science, Faculty of Advanced Life Science at Hokkaido University, Sapporo, Japan.

---

[1] Aminian, M., Bernardi, F., Camassa, R., Harris, D. M. & McLaughlin, R. M. How boundaries shape chemical delivery in microfluidics. *Science* **354**, 0532 (2016).  
 [2] Bressloff, P. C. & Newby, J. M. Stochastic models of intracellular transport. *Rev. Mod. Phys.* **85**, 135 (2013).  
 [3] Höfling, F. & Franosch, T. Anomalous transport in the crowded world of biological cells. *Reports on Progress in Physics* **76**, 046602 (2013).

[4] Ernst, D., Hellmann, M., Köhler, J. & Weiss, M. Fractional brownian motion in crowded fluids. *Soft Matter* **8**, 4886–4889 (2012).  
 [5] Tolić-Nørrelykke, I. M., Munteanu, E.-L., Thon, G., Oddershede, L. & Berg-Sørensen, K. Anomalous diffusion in living yeast cells. *Physical Review Letters* **93**, 078102 (2004).  
 [6] Shen, H. *et al.* Single particle tracking: from theory to biophysical applications. *Chemical reviews* **117**, 7331–7376 (2017).  
 [7] Wang, B., Anthony, S. M., Bae, S. C. & Granick, S. Anomalous yet brownian. *Proceedings of the National Academy of Sciences* **106**, 15160–15164 (2009).  
 [8] Wang, B., Kuo, J., Bae, S. C. & Granick, S. When brownian diffusion is not gaussian. *Nature materials* **11**, 481–485 (2012). Publisher: Nature Publishing Group.  
 [9] Skaug, M. J., Mabry, J. & Schwartz, D. K. Intermittent molecular hopping at the solid-liquid interface. *Phys. Rev. Lett.* **110**, 256101 (2013).  
 [10] Leptos, K. C., Guasto, J. S., Gollub, J. P., Pesci, A. I. & Goldstein, R. E. Dynamics of enhanced tracer diffusion in suspensions of swimming eukaryotic microorganisms. *Physical Review Letters* **103**, 198103 (2009).  
 [11] Chakraborty, I., Rahamim, G., Avinery, R., Roichman, Y. & Beck, R. Nanoparticle mobility over a surface as a probe for weak transient disordered peptide–peptide interactions. *Nano Letters* **19**, 6524–6534 (2019).  
 [12] Guan, J., Wang, B. & Granick, S. Even hard-sphere colloidal suspensions display fickian yet non-gaussian diffusion. *ACS nano* **8**, 3331–3336 (2014).  
 [13] Chakraborty, I. & Roichman, Y. Disorder-induced fickian, yet non-gaussian diffusion in heterogeneous media. *Physical Review Research* **2**, 022020 (2020).  
 [14] Chubynsky, M. V. & Slater, G. W. Diffusing diffusivity: A model for anomalous, yet brownian, diffusion. *Physical Review Letters* **113**, 098302 (2014).  
 [15] Yamamoto, E., Akimoto, T., Mitsutake, A. & Metzler, R. Universal relation between instantaneous diffusivity and radius of gyration of proteins in aqueous solution. *Physical Review Letters* **126**, 128101 (2021).  
 [16] Barkai, E. & Burov, S. Packets of diffusing particles exhibit universal exponential tails. *Physical Review Letters* **124**, 060603 (2020).  
 [17] Chechkin, A. V., Seno, F., Metzler, R. & Sokolov, I. M. Brownian yet non-gaussian diffusion: from superstatistics to subordination of diffusing diffusivities. *Physical Review X* **7**, 021002 (2017).  
 [18] Sposini, V., Chechkin, A. & Metzler, R. First passage statistics for diffusing diffusivity. *J. Phys. A: Math Theor* **52**, 04LT01 (2018).  
 [19] Lanoiselée, Y., Moutal, N. & Grebenkov, D. S. Diffusion-limited reactions in dynamic heterogeneous media. *Nature communications* **9**, 1–16 (2018).  
 [20] Lanoiselée, Y. & Grebenkov, D. S. A model of non-gaussian diffusion in heterogeneous media. *Journal of Physics A: Mathematical and Theoretical* **51**, 145602 (2018).  
 [21] Jain, R. & Sebastian, K. L. Diffusion in a crowded, rearranging environment. *The Journal of Physical Chemistry B* **120**, 3988–3992 (2016).  
 [22] Jain, R. & Sebastian, K. L. Diffusing diffusivity: survival in a crowded rearranging and bounded domain. *The Journal of Physical Chemistry B* **120**, 9215–9222 (2016).

- [23] Han, Y. *et al.* Brownian motion of an ellipsoid. *Science* **314**, 626–630 (2006).
- [24] Czajka, P., Antosiewicz, J. M. & Długosz, M. Effects of hydrodynamic interactions on the near-surface diffusion of spheroidal molecules. *ACS omega* **4**, 17016–17030 (2019).
- [25] Matse, M., Chubynsky, M. V. & Bechhoefer, J. Test of the diffusing-diffusivity mechanism using near-wall colloidal dynamics. *Physical Review E* **96**, 042604 (2017).
- [26] Serov, A. S. *et al.* Statistical tests for force inference in heterogeneous environments. *Scientific Reports* **10**, 1–12 (2020).
- [27] Frishman, A. & Ronceray, P. Learning force fields from stochastic trajectories. *Physical Review X* **10**, 021009 (2020).
- [28] Lavaud, M., Salez, T., Louyer, Y. & Amarouchene, Y. Stochastic inference of surface-induced effects using brownian motion (2021).
- [29] See Supplemental Material at [URL will be inserted by publisher] for further experimental numerical and analytical details.
- [30] Barton, N. On the method of moments for solute dispersion. *Journal of Fluid Mechanics* **126**, 205–218 (1983).
- [31] Biswas, R. R. & Sen, P. N. Taylor dispersion with absorbing boundaries: A stochastic approach. *Physical Review Letters* **98**, 164501 (2007).
- [32] Vedel, S., Hovad, E. & Bruus, H. Time-dependent Taylor–Aris dispersion of an initial point concentration. *Journal of fluid mechanics* **752**, 107–122 (2014).
- [33] Guérin, T. & Dean, D. S. Force-induced dispersion in heterogeneous media. *Physical Review Letters* **115**, 020601 (2015).
- [34] Guérin, T. & Dean, D. S. Kubo formulas for dispersion in heterogeneous periodic nonequilibrium systems. *Physical Review E* **92**, 062103 (2015).
- [35] Vilquin, A. *et al.* Time dependence of advection-diffusion coupling for nanoparticle ensembles. *Phys. Rev. Fluids* **6**, 064201 (2021).
- [36] Brenner, H. & Edwards, D. A. *Macrotransport Processes* (Butterworth-Heinemann, 1993-08-31). Google-Books-ID: Hno04ngQPAYC.
- [37] Mercer, G. & Roberts, A. A complete model of shear dispersion in pipes. *Japan journal of industrial and applied mathematics* **11**, 499–521 (1994).
- [38] Balakotaiah, V., Chang, H.-c. & Smith, F. Dispersion of chemical solutes in chromatographs and reactors. *Philosophical Transactions of the Royal Society of London. Series A: Physical and Engineering Sciences* **351**, 39–75 (1995).
- [39] Marbach, S. & Alim, K. Active control of dispersion within a channel with flow and pulsating walls. *Physical Review Fluids* **4**, 114202 (2019).
- [40] Alexandre, A., Guérin, T. & Dean, D. S. Generalized Taylor dispersion for translationally invariant microfluidic systems. *Phys. Fluids* **33**, 082004 (2021).
- [41] Lau, A. W. & Lubensky, T. C. State-dependent diffusion: Thermodynamic consistency and its path integral formulation. *Physical Review E* **76**, 011123 (2007).
- [42] Avni, Y., Komura, S. & Andelman, D. Brownian motion of a charged colloid in restricted confinement. *Physical Review E* **103**, 042607 (2021).
- [43] Lavaud, M., Salez, T., Louyer, Y. & Amarouchene, Y. Stochastic inference of surface-induced effects using brownian motion. *Physical Review Research* **3**, L032011 (2021).
- [44] Israelachvili, J. N. *Intermolecular and surface forces, second edition* (Academic press, London, 1991).
- [45] Brenner, H. The slow motion of a sphere through a viscous fluid towards a plane surface. *Chemical Engineering Science* **16**, 242–251 (1961).
- [46] Faxen, H. Die bewegung einer starren kugel langs der achse eines mit zäher flüssigkeit gefüllten rohres. *Arkiv for Matematik Astronomi och Fysik* **17**, 1–28 (1923).
- [47] Bevan, M. A. & Prieve, D. C. Hindered diffusion of colloidal particles very near to a wall: Revisited. *The Journal of Chemical Physics* **113**, 1228–1236 (2000).